A bone marrow ECM mimicking, animal-component free hydrogel identifies TNTs as key mediators of druggable cell-cell and cell-ECM crosstalk in an animal replacement organoid model.

Hockney, Sean[1], Parker, Jess[1], Tzivelekis, Babis[3], Blair Helen[2], Dalgarno, Kenny[3] and Pal, Deepali[1,2]*

*Correspondence to Pal,D. at deepali.pal@northumbria.ac.uk

Affiliations

[1] Department of Applied Sciences, Northumbria University, Newcastle upon Tyne, NE1 8ST. UK.

[2] Wolfson Childhood Cancer Research Centre, Translational and Clinical Research Institute, Faculty of Medical Sciences, Newcastle University, Herschel Building Level 6, Brewery Lane, Newcastle upon Tyne, NE1 7RU. UK.

[3] School of Engineering, M18A, Stephenson Building, Newcastle University, Newcastle upon Tyne, NE1 7RU

Abstract

Improved and low toxicity treatments are urgently required to treat cancers, however cancer drug development is hindered by high drug attrition rates. Lack of tractable, reproducible, and transferrable platforms are key impediments hindering cancer drug development. Here we develop a prototype ECM, Vitronectin-Alginate-Laminin (VAL), comprised of animal free components, in defined formulations. We perform an in-depth analysis of the physical, chemical, and biological parameters of VAL and using acute lymphoblastic leukaemia (ALL) as a paradigm, optimise development of VAL-mesenchymal stroma cells (MSC)-ALL organoids. We show engraftment of patient derived leukaemia samples within our MSC-VAL organoids and find that ALL-interactions with both ECM and MSC mediate leukaemia biology. Ultimately, we show tractability of our model to study cell-cell crosstalk – we apply our model to reveal formation of TNTs between both MSC and patient-derived ALL in cells that have escaped anti-leukaemia treatment.

Introduction

Next generation organoid models have come a long way, especially in recent times and their importance as human relevant systems with potential to replace animal testing has become increasingly prominent [1]. The importance of such models has gained significant attention since the Food and Drug Administration's (FDA's) recent announcement that it will no longer be a requirement for all drugs to be tested on animals prior to in-human trials. Indeed, the FDA itself has now committed to finding new human relevant and non-animal technologies to replace the use of laboratory animals in the development of new drugs and products.

Clinically relevant and human-based non animal technologies are especially warranted in haematological malignancies, where the role of microenvironment is of major significance and furthermore, transferrable, defined and reproducible co-culture [2], spheroid and organoid [3, 4] models to efficiently capture leukaemia-niche communications are still emerging. Despite significant advances in

human cell-based technologies and state-of-the-art organoid platforms [5], a key limitation remains lack of appropriate extra cellular matrices (ECM) that are defined in composition, amenable to scalable approaches such as 3D bioprinting and are devoid of animal-derived components such as Matrigel.

Besides the innovation of non-animal technologies and their detailed characterisation to validate their physiological relevance, a key pre-requisite that would determine their endorsement by the academic and pharmaceutical sector is the tractability of these models, so they can be meaningfully utilised in studying complex biology such as cell-cell crosstalk, cell-cell signalling and other intricate biology involving the extracellular matrix. To do this, here we develop a leukaemia-MSC organoid platform using a prototype animal component free and defined ECM using alginate as a neutral base. The role of laminin and vitronectin in the bone marrow haematopoietic niche is well established [6-12], here we infuse our alginate base with defined concentrations of vitronectin and laminin to develop the Vitronectin-Alginate-Laminin (VAL) biogel. Following in-depth physical and chemical characterisation we assess the function of VAL in supporting MSC and patient derived acute lymphoblastic leukaemia (ALL) cells to form MSC-ALL organoids and reveal potential druggable MSC-ALL cross-communication channels formed by leukaemia cells evading therapy.

Results

A prototype animal free alginate-based biogel enhanced with bone marrow extracellular matrix components laminin and vitronectin (VAL) shows high durability to sheer stress.

The human bone marrow is comprised of both cellular and extra-cellular matrix (ECM) components, which are essential for the proper functioning of haematopoietic cells, MSC, osteoblasts and other key cellular constituents of the haematopoietic niche [13-16]. To mimic some of the key ECM components ex vivo, we develop a prototype animal component free, alginate-based hydrogel incorporated with rh-laminin-521 and XF-vitronectin. Fourier transform infrared (FTIR) spectroscopy (Figure 1.A.) shows IR absorption bands for COO bonds at 1414 cm-1 and 1600 cm-1, CHO (C=O) bond at 1735 cm-1, C-H bonds at 2850 cm-1 and 2920 cm-1. In addition, an amide III (N-H) bond at 1470 cm-1, indicates incorporation of proteins such as laminin and vitronectin within the hydrogel.

Via scanning electron microscopy (SEM) imaging of alginate-laminin biogel, we show laminin matrix incorporation within alginate gel, and formation of tubule-like structures anchoring the laminin within the biogel (Figure 1.B.). Furthermore, through additional SEM images we find textured particles within VAL biogel (Figure.1.C), suggesting incorporation of vitronectin within VAL.

To define viscoelastic properties of VAL gel we perform rotational rheological measurements and find an increase in complex viscosity with angular frequency. We find that with increasing angular frequency or sheer strain, loss modulus, which describes the viscosity of the gel, remains unchanged and storage modulus, which describes the stiffness of the gel, increases with increasing angular frequency (Figure.1.C). At all times storage modulus remains higher than loss modulus. These data substantiate viscoelastic properties of VAL and indicate that the gel retains structure despite increasing sheer stress.

VAL biogel supports proliferation of primary human mesenchymal stroma cells over a 14-day period.

We assessed the ability of VAL biogel to support the proliferation of primary human bone marrow derived MSC cultures over medium term periods. In the first instance we show MSC forming cell aggregates and

interacting with VAL biogel (Figure 2.A.). Subsequent cell counts taken at start of cultures (day 0) and then day 1 and day 14 show that VAL biogels sustain starting MSC counts and furthermore, we show nearly two-fold increase in cell counts within VAL biogels on day 14 (Figure 2.B.). In addition, we perform live cell imaging using hoechst dye to stain the nucleus and actin to stain cytoskeleton (Figure 2.C.). Here we find that MSC form spheroid-like aggregates within VAL biogel.

Patient derived leukaemia-VAL organoids upregulate key anti-apoptosis oncogene BCL2, along with cell-adhesion molecule N-Cadherin (CDH2).

We assessed if VAL biogel is able to engraft and sustain growth of patient derived ALL cells over long time periods, that is, in cultures extending over 14 days. In the first instance, we explore if patient derived ALL cells would engraft within VAL, and interact with vitronectin and laminin components within VAL. We seed ALL cell suspension in cultures surrounding acellular VAL gels and find that after seven days of seeding, leukaemia cells migrate to and seed within VAL. Furthermore, we find that ALL cells form aggregates within VAL and these cell aggregates bind to laminin and interact with vitronectin (Figure.3.A-C). Using samples from 5 different patients at diagnosis and a sample from a patient at relapse, we further show that patient derived ALL cells proliferate significantly more in 3D VAL organoid cultures compared to suspension cultures (Figure.3.D-I). In a previous study we had discovered that bone marrow niche primed patient derived leukaemia cells upregulated CDH2, and that CDH2-mediated leukaemia-niche interactions was druggable via ADH-1 [16, 17]. Here, we find that patient derived leukaemia cells harvested following a seven-day VAL culture upregulate the anti-apoptotic oncogene BCL2 (Figure 3.J.), cell adhesion molecule CDH2 (Figure.3.K.) and downregulate another BCL2 family of apoptotic gene, namely MCL1(Figure.3.L.).

Patient derived leukaemia cell interaction with vitronectin and laminin within VAL biogel leads to increased fraction of quiescent cells following dexamethasone treatment.

Dormant and quiescent cancer cells play a key in treatment resistance and relapse [14, 16]. However, isolation of patient derived dormant leukaemia cells generally involve mouse serial transplantation assays, which are lengthy experiments and use a lot of animals [14]. Therefore, we next evaluate if VAL is able to support engraftment of G0, quiescent

leukaemia cells. To do this we seed patient derived leukaemia cells in suspension culture around a cross-linked VAL biogel and following a five-day culture harvest VAL-primed leukaemia cells for subsequent G0/G1 analysis. We find that VAL-primed leukaemia cells that did not migrate within the biogel possess a lower fraction of G0 cells (G0 = 7%, Figure.4.A.) compared to VAL-primed leukaemia cells that had migrated and were encased within VAL biogel (G0 = 10%, Figure.4.C.). Furthermore, we find that under dexamethasone treatment pressure there was a two-fold increase in G0 cells seen in VAL-primed leukaemia cells that had not migrated to within the biogel but remained in suspension(Figure.4.B). However, leukaemia cells that had successfully migrated and encased within VAL, possess even higher, that is, twice as many G0 cells compared to treated leukaemia cells in suspension around VAL(Figure.4.D). Together these data, corroborate the importance of extracellular matrix components in regulating leukaemia cell engraftment and furthermore, treatment resistance and dormancy. These data further substantiate the role of our animal-component free biogel in supporting G0 and treatment resistant leukaemia cells.

Dexamethasone resistant patient derived leukaemia cells form cellular protrusions and TNT in 3D ALL-organoids, to reach out to treatment sensitive cells that have escaped dexamethasone treatment.

Next, we aim to explore mechanisms of cell-cell cross-talk within VAL. We tag patient derived leukaemia cells from a diagnostic and matched relapse sample where the leukaemia cells have gained resistance against dexamethasone via a homozygous deletion of the NR3C1, glucocorticoid receptor, with TNT-staining dyes. We observe that leukaemia cells from both sample at diagnosis and relapse attach and adhere to each other, forming cell clumps (Figure.5.A-B.). Moreover, we find that following dexamethasone treatment, resistant leukaemia cells from the relapse sample form cellular protrusions and TNT towards neighbouring treatment sensitive leukaemia cells from the diagnostic sample (Figure.5.C-D.).

MSC incorporated within VAL support greater proliferation and greater treatment resistance in patient derived leukaemia cells.

Here we show that when patient derived leukaemia cells are seeded around MSC-VAL organoids, then leukaemia cells migrate to and

engraft within these organoids. SEM images show ALL cell aggregates adhering and interacting with MSC via direct cell-cell contact and furthermore via formation of elongated TNT-like structures (Figure.6.A.). We further confirm leukaemia cell migration towards MSC-spheroids encased within VAL, where we show leukaemia cells directly attach to the MSC-spheroids (Figure.6.B.). Furthermore, we show that ALL proliferation is superior in 3D MSC-VAL organoids compared to 2D suspension cultures (Figure.6C.). We also find that leukaemia cells show reduced sensitivity to dexamethasone treatment within MSC-ALL-VAL organoids compared to ALL-VAL organoids (Figure 6.D.)

Patient derived ALL cells form tunnelling nanotubules in 3D co-culture with human mesenchymal stem cells under dexamethasone treatment pressure.

We now aim to explore mechanisms of leukaemia-MSC cross-talk in cells that survive dexamethasone treatment(Figure 7). Consistent with our previous findings, we observe that in the absence of treatment leukaemia cells migrate to and attach to MSC-spheroids within VAL. However, we find that when treated with dexamethasone then in addition to direct cell contact between MSC-ALL, TNT communication channels begin to form in co-cultures and these are formed between MSC-MSC, ALL-ALL and ALL-MSC. Together these data suggest that VAL facilitates leukaemia-MSC co-cultures, and furthermore, scrutiny of cell-cell crosstalk including direct cell-cell and cell-ECM contact as well as cell-cell communication via TNTs.

Discussion

Here we develop a prototype animal component-free, defined bone marrow ECM mimicking biogel, VAL. We perform in-depth physical, chemical and biological characterisation of VAL and show that it is successfully infused with laminin and vitronectin, key proteins within the human bone marrow microenvironment. Furthermore, we show that VAL successfully supports proliferation of MSC and engraftment of patient-derived leukaemia cells both individually and in co-cultures. We find that cancer-niche crosstalk is facilitated via both direct cell-cell contact and in the presence of dexamethasone treatment via TNT.

The role of the malignant bone marrow microenvironment in supporting the survival, growth and treatment resistance of leukaemia is well documented [13-18]. Particularly it is well known that the cancerous bone marrow niche is dynamic, its dynamism is reliant on both evolution of leukaemia growth and treatment-driven altered biology [13, 18, 19]. The altered cancer and its niche both deter healthy haematopoiesis and competent immune function in advanced and treatment refractory disease [13, 20].

Several mechanisms have been proposed to be culpable in niche-driven treatment resistance. Stroma signalling, direct cell-cell contact are some key factors mediating leukaemia growth, dormancy and treatment resistance [16, 17, 21]. However, means of clinically targeting such communications remain obscure. TNTs have recently gained importance as key mediators of cancer-niche communications. TNTs can function as a form of organelle transfer between leukaemia and stroma cells, potentially leading to treatment resistance [22, 23]. The cell adhesion molecule CDH2 is known to play a role in TNT formation and development [24, 25], and CDH2 mediated niche-leukaemia interactions are amenable to clinical targeting, for

example, via ADH-1 [16, 17], a drug that showed a well-accepted toxicity profile in Phase I solid tumour trials [17, 26]. Here, using our proof-of-concept, well defined, animal-component free MSC-ALL organoid model we find that ALL engrafted within the VAL upregulate CDH2 and furthermore, both ALL and MSC form TNTs when MSC-ALL-VAL are treated with dexamethasone.

Although we show key advances in developing a defined, reproducible, animal component-free niche-leukaemia technology, our study has limitations. The bone marrow niche is multicellular and besides the mesenchymal niche also has sinusoidal and immune niche components, incorporating of all these aspects are important to faithfully mimic leukaemia-niche crosstalk in order to reveal druggable pathways and explore biology-driven therapeutic opportunities. Furthermore, high throughput drug screening platforms require scalable approaches to yield drug dose response data within quick turnaround times. Nevertheless, here we develop a prototype MSC-ALL organoid platform which will begin innovation of defined, xeno-free next generation organoids which can be applied in widespread applications ranging potentially from scalable drug screens to human relevant platforms for the purposes of target discovery and exploration of druggable niche-driven leukaemia biology.

Methods:

1. Developing cellular VAL gels

A biogel made of 4% vitronectin and 10% laminin was used along with an alginate base to produce final formulation of VAL biogel. Appropriate volume of VAL mixture added to cultureware and 1:1 volume crosslinking agent (calcium chloride) added to VAL and mixed using gentle pipetting. Biogel was allowed to crosslink at 37°C, 5% CO2 for 20 mins. ALL PDX cells harvested and resuspended at $1x10^6$ cells/ml in fresh culture media. Cell suspension added around biogel following the crosslinking.

2. Developing VAL gel MSC-ALL organoids

Biogel as described above added to cultureware. MSC cells harvested to a density of $0.1x10^6$ cells/model. Cells were centrifuged at 1500rpm for 5 minutes to remove media. Pellet was resuspended in equivalent volume of crosslinking agent. MSC-crosslinking agent suspension pipetted into model, and gently mixed to distribute cells evenly throughout model. VAL-MSC models incubated for 20 mins at 37°C, 5% CO2 to crosslink biogel. ALL cells added to crosslinked VAL-MSC models as described in 1.

3. DiO-Dil staining of MSC-ALL organoids, treated and untreated

PMSC and ALL harvested from 2D culture at density of 0.1x106 cells/model and 1x106 cells/model respectively. Cells were resuspended at a density of 1x106 cells/ml in fresh serum-free media. 5µl/ml cell suspension of cell labelling solution (DiO for MSC, Dil for ALL) was added and mixed well by gentle pipetting. Cells and staining

solution were incubated at 37°C, 5% CO2 for 20 minutes. Cells were then centrifuged at 1500rpm for 5 mins, supernatant removed, pellet resuspended in fresh serum-free media and centrifuged again at same speed and for same time. This process was repeated twice. Following final centrifugation, PMSC and ALL cell pellets were combined and resuspended in volume of crosslinker equivalent to VAL volume. MSC-ALL organoids were left to crosslink for 20 minutes at 37°C and 5% CO2 before fresh culture media was added. Control models had 1ml media added per model, treated models had 1ml media added with 10nM dexamethasone. Models were incubated at 37°C, 5% CO2 for 90 minutes before imaging.

4. CellMask Actin Tracking Solution and Hoechst staining of MSC-ALL organoids

PMSC and ALL harvested from 2D culture at density of 0.1x106cells/model and 1x106 cells/model respectively. VAL gel MSC-ALL organoids made as described in 2. 1x CellMask Actin staining solution made from 1000x staining solution using live-cell compatible media. Sufficient 1x CellMask actin solution added to model, enough to cover model. Models were incubated for 60 minutes at 37°C, 5% CO2. CellMask actin solution removed from model and 1x Hoechst solution added, enough volume to cover model. Models incubated for 30 mins before 4 rinsing steps with fresh media. Models imaged.

5. Patient derived acute lymphoblastic leukaemia (ALL) cells

Patient-derived xenografts (PDX) were generated as previously described [16]. Male and female 8-12 weeks old mice, immunocompromised NOD.Cg-PrkdcscidIl2rgtm1Wjl/SzJ (NSG) from an in-house colony were transplanted with $1x10^6$ viable patient or PDX ALL cells by intrafemoral injection. Mice were group housed in specific pathogen-free barrier conditions with a 12hour light/dark cycle. PDX ALL blasts cells were isolated from spleen of engrafted humanely euthanized NSG mice when either, high levels of blast were detected

by flow cytometry in the peripheral blood or health signs such as anaemia, weight loss and loss of muscle tone were first observed. All regulated animal procedures were approved by the Animal Welfare and Ethical Review Board of Newcastle University and conducted in accordance with the Animals (Scientific Procedures) Act 1996 under the UK Home Office licence P74687DB5.

References:

1. Hockney, S., et al., *Next generation organoid engineering to replace animals in cancer drug testing.* Biochem Pharmacol, 2023. **213**: p. 115586.
2. Pal, D., et al., *Long-term in vitro maintenance of clonal abundance and leukaemia-initiating potential in acute lymphoblastic leukaemia.* Leukemia, 2016. **30**(8): p. 1691-700.
3. Wilson, A., et al., *A human mesenchymal spheroid prototype to replace moderate severity animal procedures in leukaemia drug testing [version 1; peer review: 2 approved with reservations].* F1000Research, 2022. **11**(1280).
4. Balandrán, J.C., et al., *Patient-Derived Bone Marrow Spheroids Reveal Leukemia-Initiating Cells Supported by Mesenchymal Hypoxic Niches in Pediatric B-ALL.* Front Immunol, 2021. **12**: p. 746492.
5. Khan, A.O., et al., *Human Bone Marrow Organoids for Disease Modeling, Discovery, and Validation of Therapeutic Targets in Hematologic Malignancies.* Cancer Discovery, 2023. **13**(2): p. 364-385.
6. Siler, U., et al., *Characterization and functional analysis of laminin isoforms in human bone marrow.* Blood, 2000. **96**(13): p. 4194-4203.
7. Kermani, P., et al., *Laminin Expression Is Necessary for Maintenance of the Vascular Hematopoietic Niche.* Blood, 2011. **118**(21): p. 217-217.
8. Susek, K.H., et al., *Bone marrow laminins influence hematopoietic stem and progenitor cell cycling and homing to the bone marrow.* Matrix Biology, 2018. **67**: p. 47-62.
9. Graf, F., et al., *The extracellular matrix proteins type I collagen, type III collagen, fibronectin, and laminin 421 stimulate migration of cancer cells.* The FASEB Journal, 2021. **35**(7): p. e21692.
10. Salasznyk, R.M., et al., *Adhesion to Vitronectin and Collagen I Promotes Osteogenic Differentiation of Human Mesenchymal Stem Cells.* Journal of Biomedicine and Biotechnology, 2004. **2004**: p. 169212.
11. Mathews, S., et al., *Extracellular matrix protein mediated regulation of the osteoblast differentiation of bone marrow derived human mesenchymal stem cells.* Differentiation, 2012. **84**(2): p. 185-192.
12. Goyal, U. and M. Ta, *A novel role of vitronectin in promoting survival of mesenchymal stem cells under serum deprivation stress.* Stem Cell Research & Therapy, 2020. **11**(1): p. 181.
13. Duan, C.W., et al., *Leukemia propagating cells rebuild an evolving niche in response to therapy.* Cancer Cell, 2014. **25**(6): p. 778-93.
14. Ebinger, S., et al., *Characterization of Rare, Dormant, and Therapy-Resistant Cells in Acute Lymphoblastic Leukemia.* Cancer Cell, 2016. **30**(6): p. 849-862.
15. Le, P.M., M. Andreeff, and V.L. Battula, *Osteogenic niche in the regulation of normal hematopoiesis and leukemogenesis.* Haematologica, 2018. **103**(12): p. 1945-1955.
16. Pal, D., et al., *hiPSC-derived bone marrow milieu identifies a clinically actionable driver of niche-mediated treatment resistance in leukemia.* Cell Rep Med, 2022. **3**(8): p. 100717.
17. Parker, J., et al., *Targeting N-cadherin (CDH2) and the malignant bone marrow microenvironment in acute leukaemia.* Expert Rev Mol Med, 2023. **25**: p. e16.

18. Chen, Y., et al., *Acute myeloid leukemia–induced remodeling of the human bone marrow niche predicts clinical outcome.* Blood Advances, 2020. **4**(20): p. 5257-5268.
19. Woods, K. and B. Guezguez, *Dynamic Changes of the Bone Marrow Niche: Mesenchymal Stromal Cells and Their Progeny During Aging and Leukemia.* Front Cell Dev Biol, 2021. **9**: p. 714716.
20. Barakos, G.P. and E. Hatzimichael, *Microenvironmental Features Driving Immune Evasion in Myelodysplastic Syndromes and Acute Myeloid Leukemia.* Diseases, 2022. **10**(2): p. 33.
21. Baryawno, N., et al., *A Cellular Taxonomy of the Bone Marrow Stroma in Homeostasis and Leukemia.* Cell, 2019. **177**(7): p. 1915-1932.e16.
22. Polak, R., et al., *B-cell precursor acute lymphoblastic leukemia cells use tunneling nanotubes to orchestrate their microenvironment.* Blood, 2015. **126**(21): p. 2404-14.
23. de Rooij, B., et al., *Tunneling nanotubes facilitate autophagosome transfer in the leukemic niche.* Leukemia, 2017. **31**(7): p. 1651-1654.
24. Kolba, M.D., et al., *Tunneling nanotube-mediated intercellular vesicle and protein transfer in the stroma-provided imatinib resistance in chronic myeloid leukemia cells.* Cell Death Dis, 2019. **10**(11): p. 817.
25. Chang, M., et al., *Formation of cellular close-ended tunneling nanotubes through mechanical deformation.* Science Advances, 2022. **8**(13): p. eabj3995.
26. Beasley, G.M., et al., *A phase 1 study of systemic ADH-1 in combination with melphalan via isolated limb infusion in patients with locally advanced in-transit malignant melanoma.* Cancer, 2009. **115**(20): p. 4766-74.

A

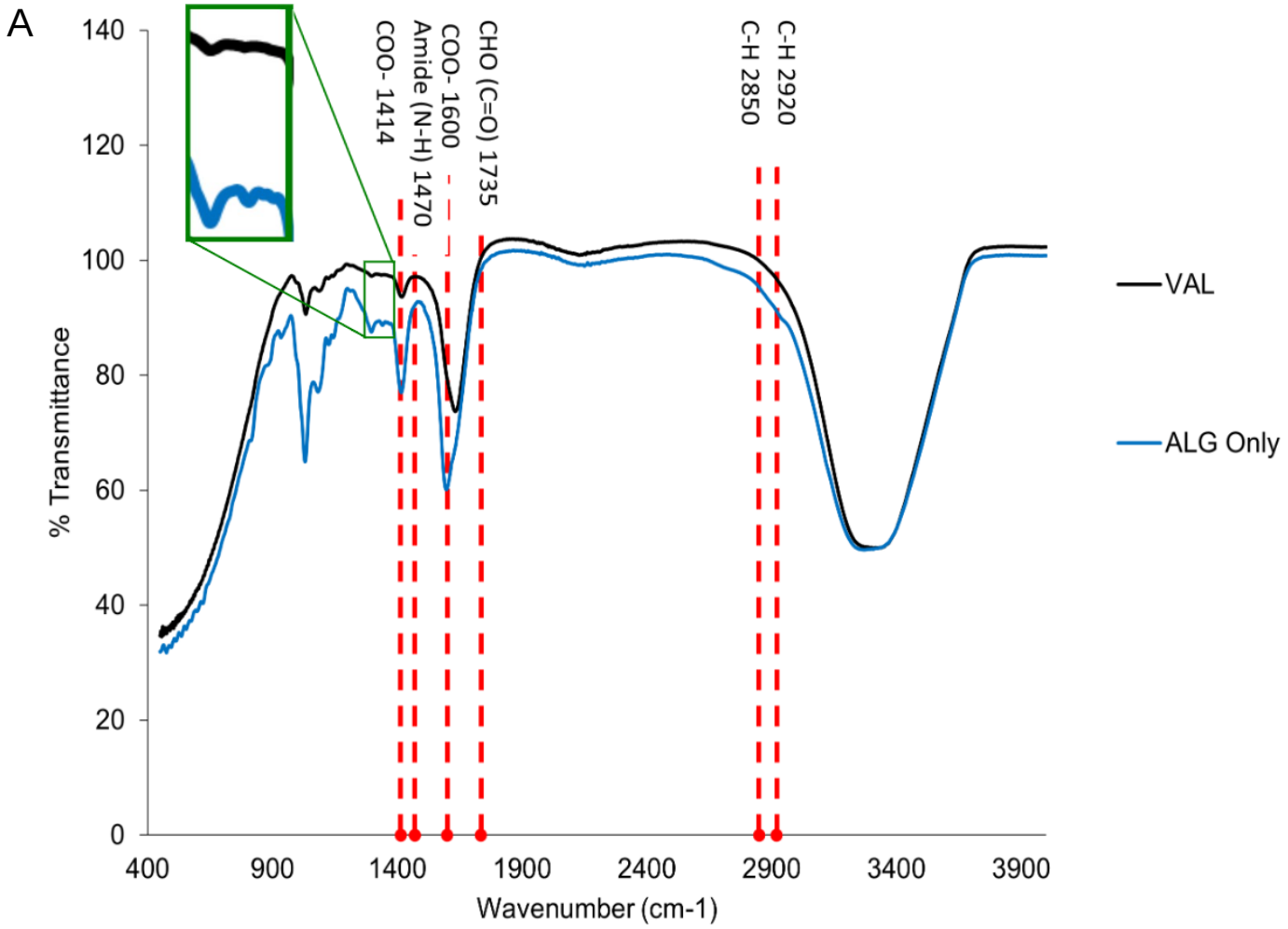
COO- 1414
Amide (N-H) 1470
COO- 1600
CHO (C=O) 1735
C-H 2850
C-H 2920
% Transmittance
Wavenumber (cm-1)
VAL
ALG Only

B

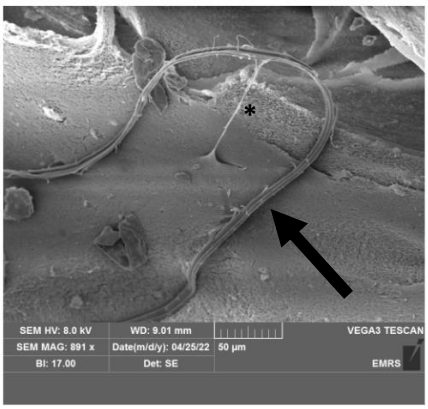
*

C

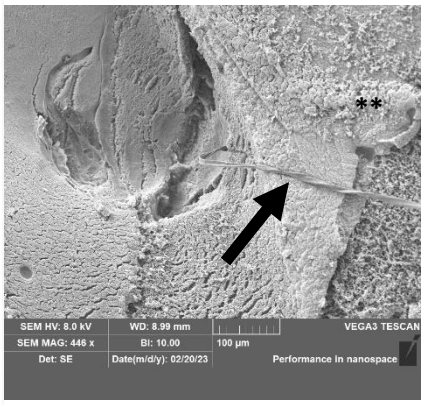
**

D

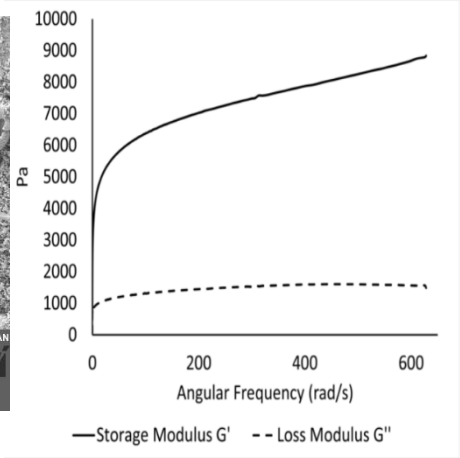
Pa
Angular Frequency (rad/s)
Storage Modulus G'
Loss Modulus G''

Figure 1: A prototype animal free alginate-based biogel enhanced with bone marrow extracellular matrix components laminin and vitronectin (VAL) shows high durability to sheer stress. A) Fourier Transform Infrared Spectroscopy (FTIR) shows incorporation of laminin into alginate biogel formulation. Peak showed in zoomed inlet in the fingerprint region of 1250-1400cm^{-1} is characteristic of laminin and present only in VAL biogel B) Scanning Electron Microscopy (SEM) of laminin (black arrow) bonded via tubule-like structures (*) with alginate in biogel. Image captured at SEM magnification of x882, BI 13, scale bar represents 50µm. C) SEM image showing laminin (black arrow) and vitronectin (**) within VAL biogel. Rheological measurements of VAL show that with increasing angular displacement, storage modulus of VAL increases and remains higher than the loss modulus.

A

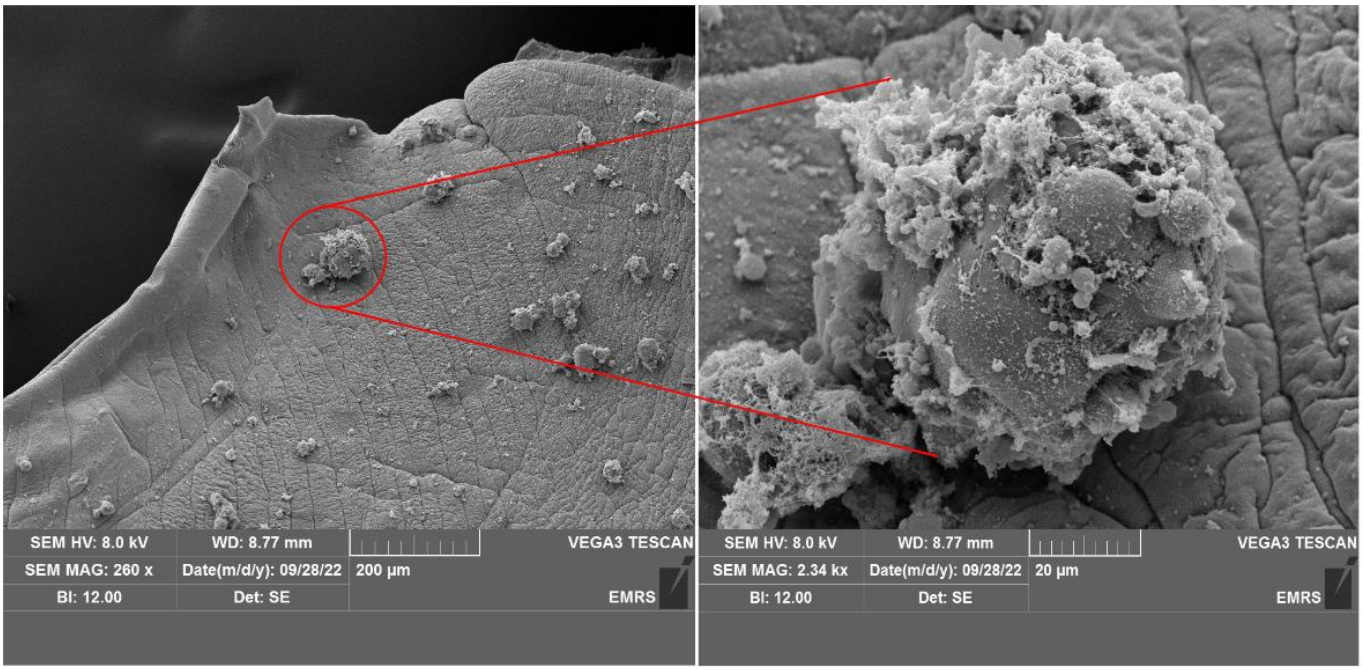
SEM HV: 8.0 kV
WD: 8.77 mm
VEGA3 TESCAN
SEM MAG: 260 x
Date(m/d/y): 09/28/22
200 µm
BI: 12.00
Det: SE
EMRS
SEM HV: 8.0 kV
WD: 8.77 mm
VEGA3 TESCAN
SEM MAG: 2.34 kx
Date(m/d/y): 09/28/22
20 µm
BI: 12.00
Det: SE
EMRS

B

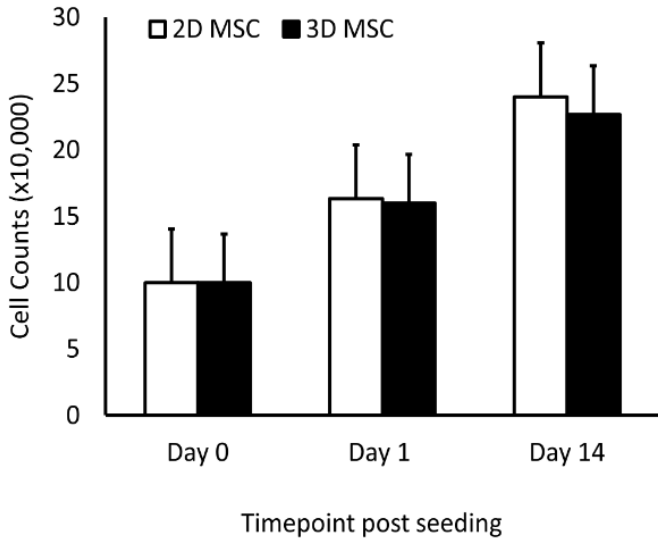
2D MSC
3D MSC
Cell Counts (x10,000)
30
25
20
15
10
5
0
Day 0
Day 1
Day 14
Timepoint post seeding

C

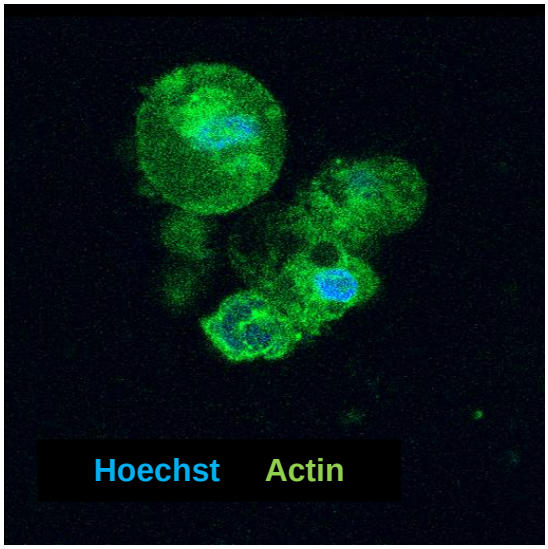
Hoechst
Actin

Figure 2: VAL biogel supports proliferation of primary human mesenchymal stem cells over a 14-day period. A) Scanning Electron Microscopy of mesenchymal stem cells within the bio-gel where cells group into small 3D clusters. Images taken at 260x magnification and zoomed inlet shows 2.34kx magnification. B) Comparable growth of MSC is seen in 2D and 3D cultures in VAL gel over a 2 week period C) Hoechst actin staining of 3D MSC spheroids within VAL gel shows aggregation of MSC into self-assembling spheroidal structures.

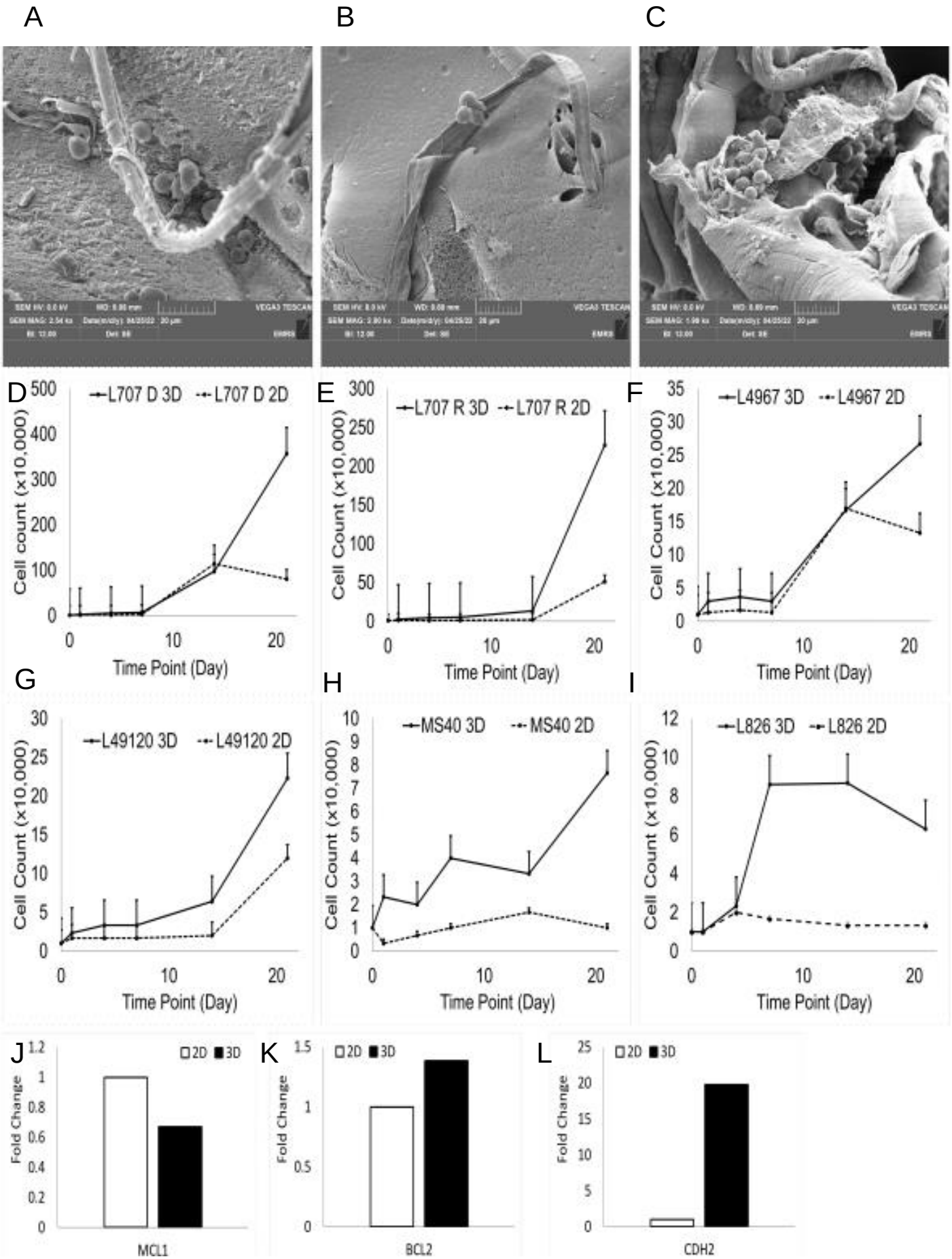
A
B
C
D
L707 D 3D
L707 D 2D
Cell count (x10,000)
Time Point (Day)
E
L707 R 3D
L707 R 2D
Cell Count (x10,000)
Time Point (Day)
F
L4967 3D
L4967 2D
Cell Count (x10,000)
Time Point (Day)
G
L49120 3D
L49120 2D
Cell Count (x10,000)
Time Point (Day)
H
MS40 3D
MS40 2D
Cell Count (x10,000)
Time Point (Day)
I
L826 3D
L826 2D
Cell Count (x10,000)
Time Point (Day)
J
2D
3D
Fold Change
MCL1
K
2D
3D
Fold Change
BCL2
L
2D
3D
Fold Change
CDH2

Figure 3: A-C) Scanning Electron Microscopy of PDX leukaemia cells incorporated within VAL biogel shows interaction between leukaemia, laminin and vitronectin. Images taken at x2.54k (A), x2.00k (B) and 1.99k (C) SEM magnification with BI of 12.00 (A and B) and 13.00 (C). Scale bar= 20µm. D-I) Growth of PDX-ALL in 2D suspension cultures versus 3D leukaemia-VAL organoids. Increased growth seen in 3D over 2D setup. SD from N=3. J-L) qPCR analysis of MCL1, BCL2 and CDH2 in 2D versus 3D PDX-ALL-organoid cultures.

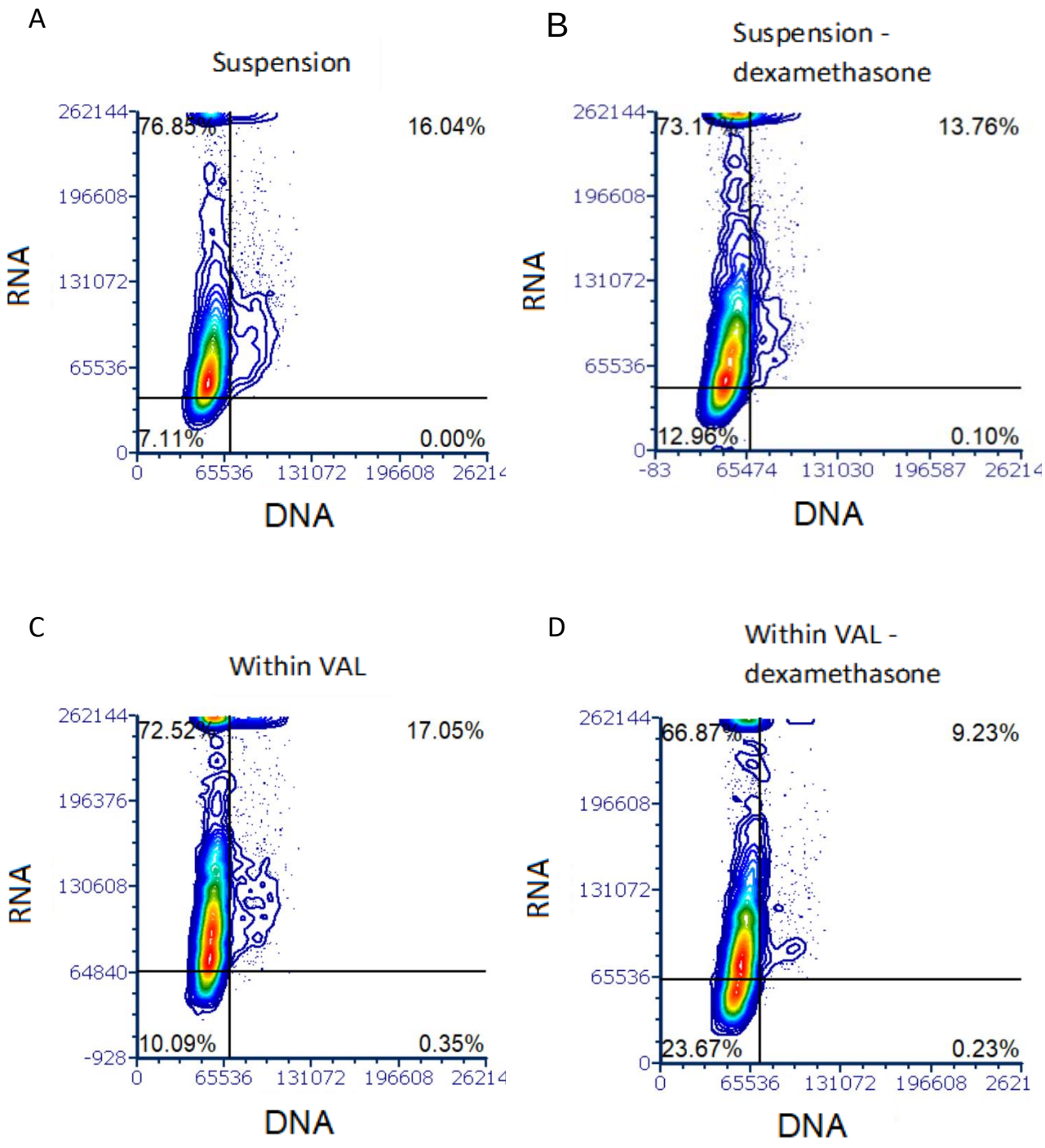
A
Suspension
76.85%
16.04%
7.11%
0.00%
262144
196608
131072
65536
0
RNA
0
65536
131072
196608
DNA
B
Suspension - dexamethasone
73.17%
13.76%
12.96%
0.10%
262144
196608
131072
65536
0
RNA
-83
65474
131030
196587
DNA
C
Within VAL
72.52%
17.05%
10.09%
0.35%
262144
196376
130608
64840
-928
RNA
0
65536
131072
196608
DNA
D
Within VAL - dexamethasone
66.87%
9.23%
23.67%
0.23%
262144
196608
131072
65536
0
RNA
0
65536
131072
196608
DNA

Figure 4: Patient derived leukaemia cell interaction with vitronectin and laminin within VAL biogel leads to increased fraction of quiescent cells following dexamethasone treatment. Here we seeded PDX-ALL in suspension around a block of acellular VAL gel. In this experimental set up “within VAL” cells refer to leukaemia cells that migrated to and remained inside the gel, and “suspension” cells refer to leukaemia cells that did not migrate within VAL but remined outside in suspension form. The treatment arm received 5nM dexamethasone over a 5-day period. A. 7% of suspension leukaemia culture are in G0/quiescent phase B. 13% of suspension leukaemia culture are in G0/quiescent phase under dexamethasone treatment C. 10% of leukaemia within VAL are in G0/quiescent phase D. 24% of leukaemia within VAL are in G0/quiescent phase under dexamethasone treatment.

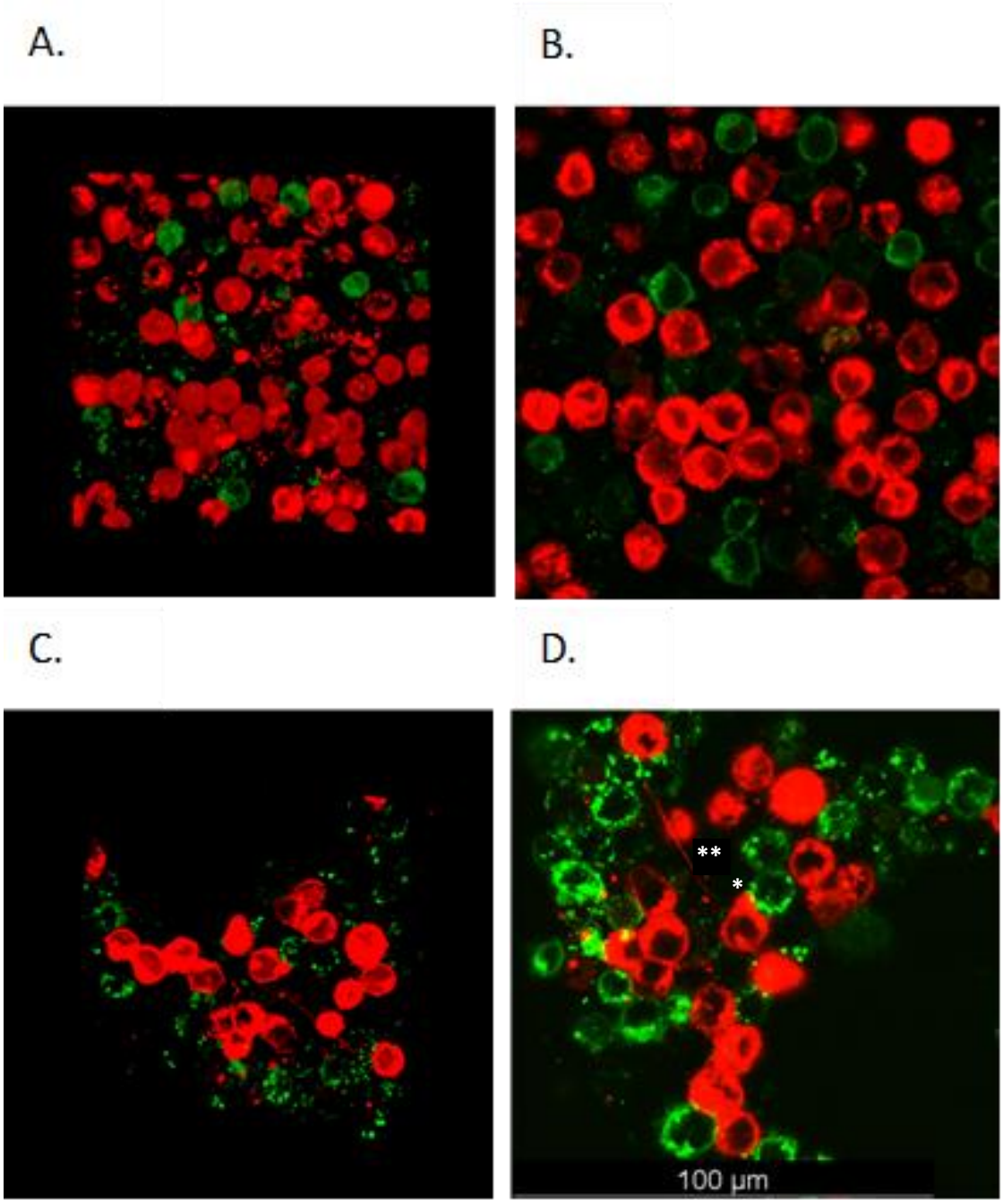
A.
B.
C.
D.
**
*
100 µm

Figure 5. Dexamethasone resistant patient derived leukaemia cells form cellular protrusions and TNT in 3D ALL-organoids, to reach out to treatment sensitive cells that have escaped dexamethasone treatment. DiO staining of dexamethasone sensitive and DiL staining of dexamethasone resistant leukaemia cells showing A. Untreated leukaemia cells, Z stack at X40 magnification B. Untreated leukaemia cells X63 magnification C. Dexamethasone treated cells, Z stack at X40 magnification D. Dexamethasone treated cells at X63 magnification. * marks cellular protrusions between treatment resistant and sensitive cells that have escaped therapy and ** marks TNT forming from treatment resistant cells. Leukaemia cells were stained with the dyes and encased within VAL and relevant organoids were treated for 3 hours and then imaged.

A.

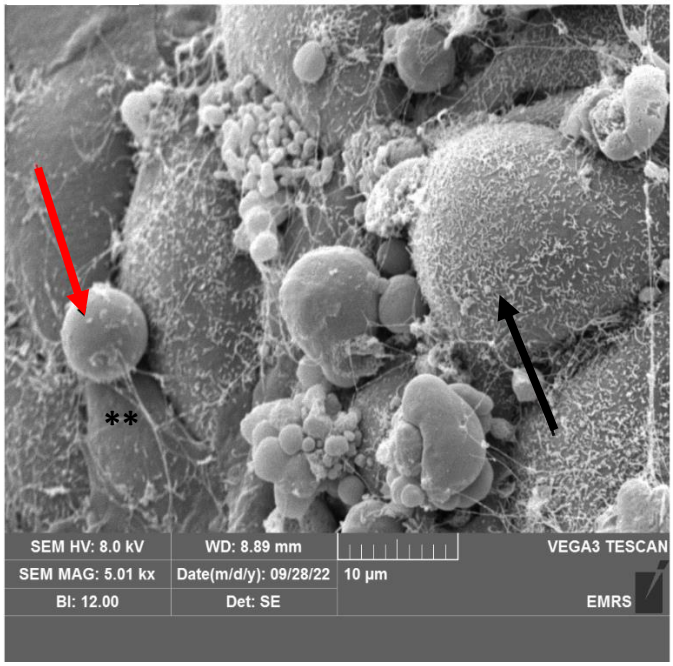
**
SEM HV: 8.0 kV
WD: 8.89 mm
VEGA3 TESCAN
SEM MAG: 5.01 kx
Date(m/d/y): 09/28/22
10 µm
BI: 12.00
Det: SE
EMRS

B.

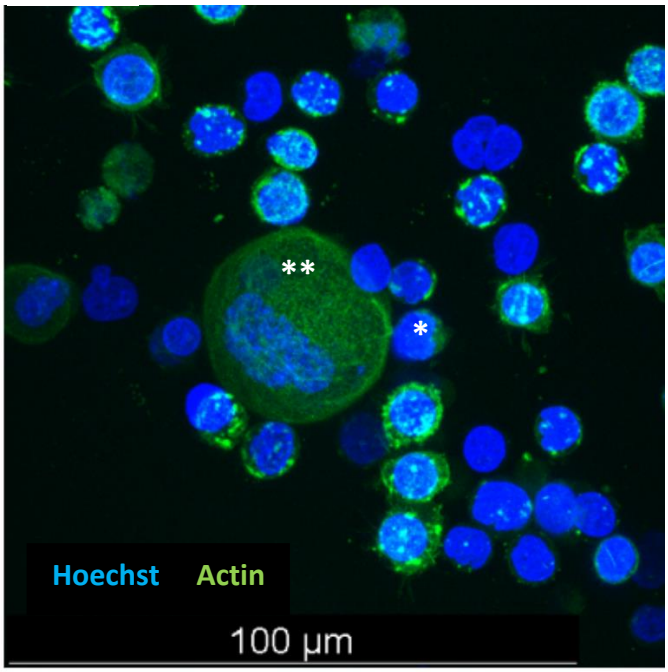
**
*
Hoechst
Actin
100 µm

C.

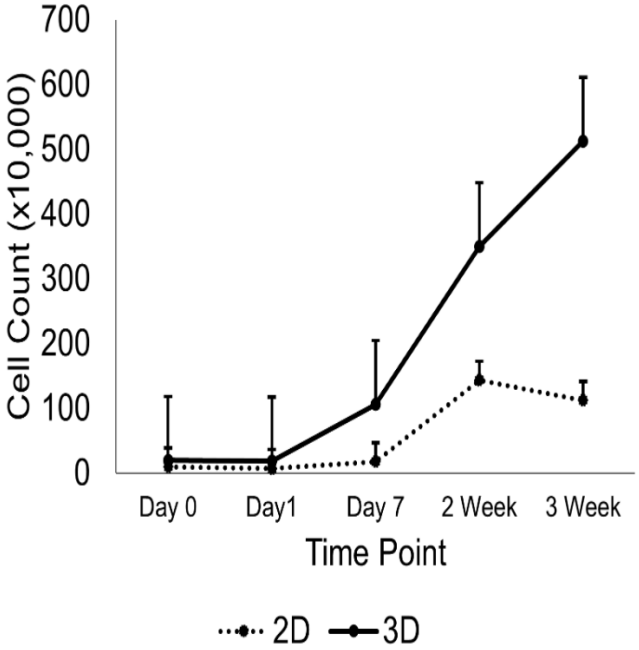
Cell Count (x10,000)
700
600
500
400
300
200
100
0
Day 0
Day1
Day 7
2 Week
3 Week
Time Point
2D
3D

D.

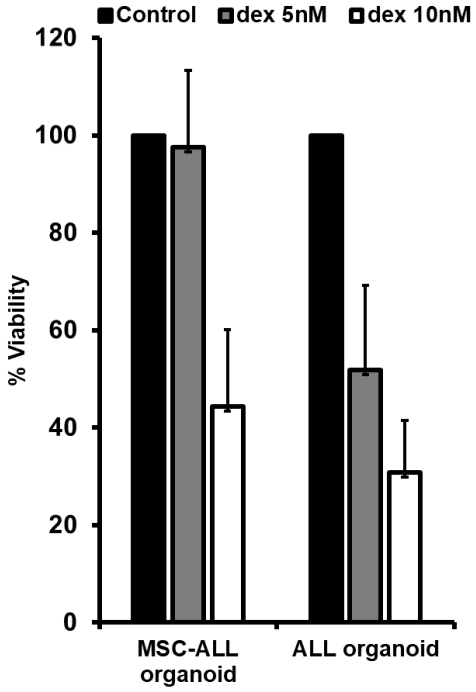
Control
dex 5nM
dex 10nM
% Viability
120
100
80
60
40
20
0
MSC-ALL organoid
ALL organoid

Figure 6: Mesenchymal stem cells incorporated within VAL support greater proliferation and greater treatment resistance in patient derived leukaemia cells. A. Scanning Electron Microscopy image showing mesenchymal stroma cells and leukaemia cells adhering with each other and forming elongated cobweb like inter-cellular tubules (indicated by **). B. Hoechst actin staining of mesenchymal stem cell self-assembling spheroids (white **) and leukaemia cells (white *) C. Cell counts of patient derived leukaemia cells following 3-week co-culture with MSC in VAL-organoids. D. % Viability of leukaemia cells following dexamethasone treatment in MSC-ALL organoids versus ALL-organoids.

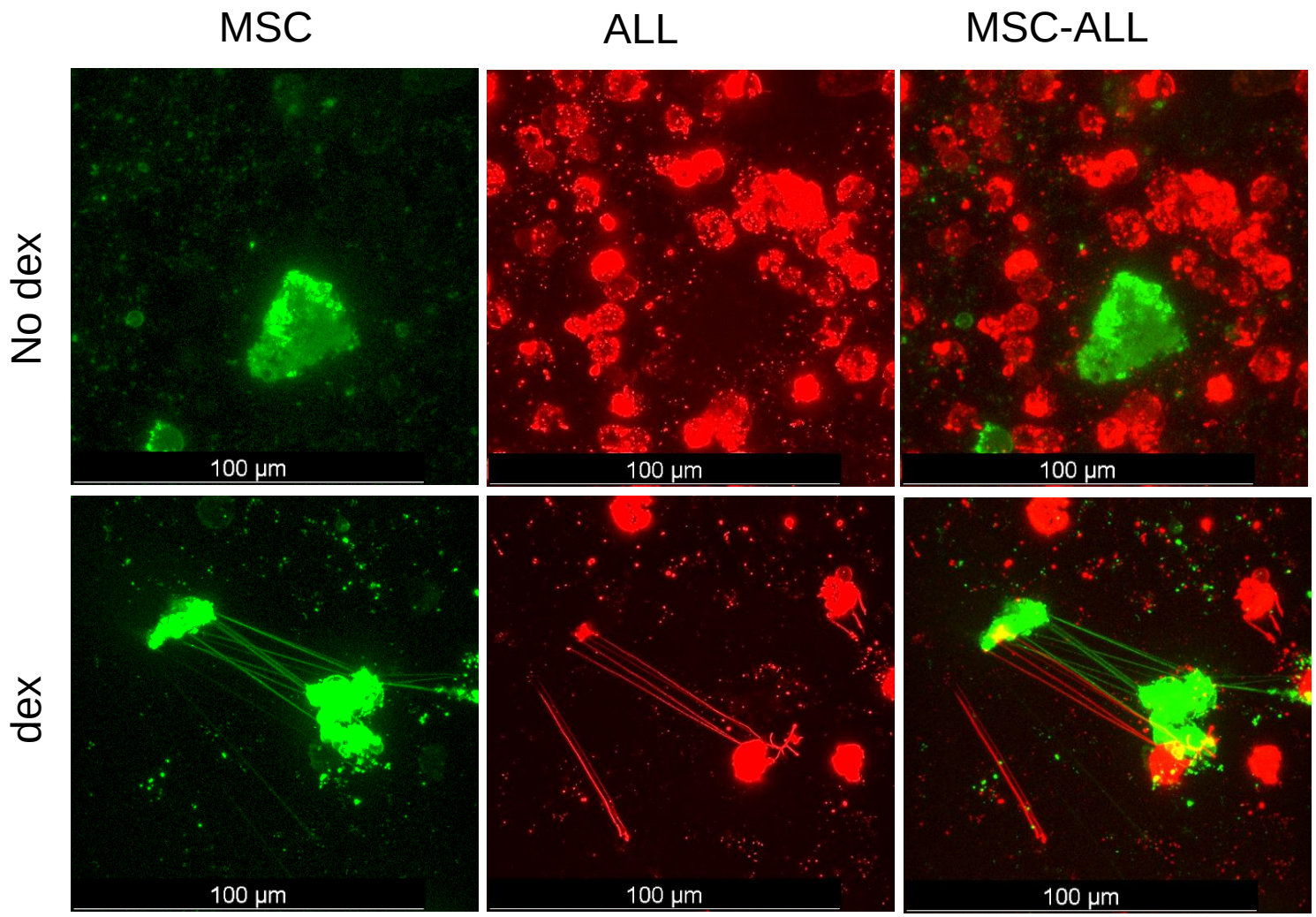
MSC
ALL
MSC-ALL
No dex
dex
100 µm
100 µm
100 µm
100 µm
100 µm
100 µm

Figure 7: Patient derived ALL cells form tunnelling nanotubules in 3D co-culture with human mesenchymal stem cells under dexamethasone treatment pressure. Mesenchymal stem cells have been stained with DiO (green) and ALL cells have been stained with DiL (red). Cells were then incorporated within VAL and relevant organoids were treated with 25 nM dexamethasone for three hours and then imaged.